https://africanjournalofbiomedicalresearch.com/index.php/AJBR
Afr. J. Biomed. Res. Vol. 27 (September 2024); 651-669

Research Article

Manufacturing and Characterization of Nitinol Shape Memory Alloy: A Comprehensive Study

Ali F. Abdulkareem[1,*], Auns Q. Al-Neami[2], and Tariq J. Mohammed[3]

[1,2]Al-Nahrain University, College of Engineering, Biomedical Engineering Department, Baghdad, Iraq*
[3]Alkarkh General Hospital, Alkarkh Health Directorate, Iraqi MOH

ABSTRACT
Nitinol-shaped memory alloy is a superplastic alloy that can return to its pre-deformed shape when heated. Different additives and manufacturing techniques resulted in different alloy characteristics. This study aims to manufacture three different concentrations of nitinol alloy using the sintering technique to expose these alloy characteristics. The alloys were manufactured using sintering techniques followed by melting in an argon atmosphere to prevent oxidation. The procedure includes preparing three concentrations of raw materials: NiTi of (45% Ti + 55% Ni), NiTiCu of (45% Ti + 35% Ni + 20% Cu), and NiTiAl of (35% Ti + 45% Ni + 20% Al), mixing them and sintering them, first directly and second after compressing them under five tons pressure, and examining their properties. Structural and thermal properties were analyzed through X-ray diffraction (XRD), energy dispersive spectroscopy (EDS), scanning electron microscopy (SEM), and differential scanning calorimeter (DSC). The results demonstrated the influence of alloying elements on the micro-structure, density, and phase transformation temperatures, which are critical for potential applications in various industries. It was found that the manufactured nickel titanium alloy shows a phase of heating transformation temperature of austenite phase starting (As) at 60.87 °C and austenite phase finishing (Af) at 75.40 °C, the NiTiCu alloy shows a phase of heating transformation temperature of As at 60.57 °C and Af at 69.69 °C, and the NiTiAl alloy shows a phase of heating transformation temperature of As at 64.10 °C and Af at 75.03 °C. The study findings indicate that the addition of copper and aluminum alters the thermal and structural characteristics of the Nitinol alloys, providing insights into their performance for specific applications.

Keywords: Shape Memory Alloy, Nitinol, NiTi, NiTiCu, NiTiAl, Sintering, XRD, DSC

**Author for correspondence: Email: st.ali.f.abdulkareem@ced.nahrainuniv.edu.iq*

Receiving Date: 10/07/2024 Acceptance Date: 20/08/2024

DOI: https://doi.org/10.53555/AJBR.v27i3.2645

Introduction

Nitinol (NiTi) Shape Memory Alloy:

One of the most promising smart materials are shape memory alloys (SMAs), especially nickel-titanium (NiTi or Nitinol). These alloys are great and desirable because of their higher dependability and behaviour compared to all other commercially available alloys. In addition, strain recovery, (Ni-Ti) is preferable for a wide application of medical uses to fabricate a specific alloy characteristic such as biocompatibility, corrosion resistance, and fatigue behaviour. NiTi is a smart material (SMA) that can return to its pre-deformed form when heated [1], [2].

General Properties of Nitinols alloy and Their Hysteresis loop:

In general, nitinol (Ni-Ti) shape memory alloys can be found in two different phases: martensite and austenite. Martensite phase formed in low temperatures, while the austenite produces in high temperatures or main phase both depending on the temperature of the crystalline structures. Both (austenitic and martensitic) NiTi have several different characteristics, like electrical resistance, damping behavior, and young modulus. While the nickel atom is located at the center of the crystallographic cube, the titanium atom can be found at each cube's eight corners,

causing the Central Cubic Structural Body (BCC) structure of the austenite. Additionally, due to its symmetrical microstructure the austenitic phase is considered as the main phase. NiTi martensite's phase is considered to have less symmetrical and lattice structure, and it has a rhombus alignment, where the atoms are located at each rhombus corners in comparison with the austenitic phase [1,3].

The hysteresis loop, which produces shape memory characteristics is related to martensitic phase transformation. Some applications of shape memory alloys need small hysteresis loops, while others require large ones. Therefore, having control over the hysteresis size is crucial. For that purpose, there are three different methods introduced to do that: The hysteresis loops in both NiTi and CuZnAl alloys were narrowed by mechanical vibration by up to 17%, but the addition of the third element such as Cu in a NiTi alloy caused the loop width to shrink by S~4 times[4].

Nitinol Alloys in Medical and Orthotic Applications:

Unique characteristics of Nitinol SMA permit minimally invasive surgery and aim to improve life quality for millions of people. The availability of novel materials such as nitinol is crucial to providing continued progress in improving lives globally. Nitinol shaped memory alloy has the potential to restore its original shape after deformation, which leads to the advancement of novel medical devices. In medical field, nitinol alloys were used popularly in varies applications due to its biocompatibility, superelasticity, and fatigue and corrosion resistance. As an example, nitinol is utilized to produce catheter tubes, dental files and arch wires, guidewires, needles, stone retrieval baskets, filters, and other surgical instruments [5] [6] [7]. The superelastic property of exhibiting constant unloading stresses over large strains is a significant feature of nitinol. Thus, the force applied by a superelastic device is not strain-dependent, as in conventional materials, but temperature related. Since body temperature is normally constant, a special device can be customized that applies constant stress to a wide range of geometries. The first product to use this characteristic was the orthodontic archwire [5,7]. Although it is still in its early stages, the market for nitinol in orthopedics is intriguing. Even so, a lot of study has been done on different corrective rods, etc. [7]. A desirable material alternative for devices utilized in clinical orthopedic applications is pseudoelastic nitinol. The material's ability to apply continuous compression during shape recovery is in good agreement with the mechanobiological elements linked to bone healing, especially in applications where joint fusion and fracture healing are involved. There are more and more orthopedic medical devices that use nitinol. Two prominent examples are intramedullary nails and staples [8]. The largest and first clinical research in orthopedic foot and ankle surgery was carried out by Schipper and colleagues with new-generation nitinol staples. Using a new generation of nitinol staples, the aim of this study was to examine the radiographic union rate following midfoot and hindfoot arthrodeses and to assess the differences in results between nitinol staple and partly threaded crossing screw constructs. An example of enlarged indications can include ankle arthrodesis, pseudo-Jones and Jones fracture fixation, tibial osteotomies, tibia fractures, double and triple arthrodeses, Lisfranc injuries, and Lapidus bunionectomy [9].

Hysteresis Effect of NiTiCu:

The investigations shows that the transformation kinetics for NiTiCu alloys and its transformation hysteresis is as follows [10]:

(M_S - A_s) NiTiCu = 20°C

(A_f - M_f) NiTiCu = 50°C

Table 1: Mechanical properties of NiTiCu SMA [10]:

No.	Mechanical Property of NiTiCu SMA	Value in
1	Elastic modulus (MPa) slope of the tangent at zero point	183×10^2
2	Elastic modulus on the plateau (MPa) slope of the linear evolution	$5{,}64\times10^2$
3	Critical stress for reorientation TC (MPa)	115
4	Length of the plateau ($rd.mm^{-1}$)	40

Incomplete Cycle on Recovery (ICR) which is a partial recovery of the transformation with at least one pause in the reverse M+P transformation is required to investigate SMART phenomenology in the stress-induced transformation. In this instance, the loop will have an inversion point at ε_{ICR}within the reversion plateau and a start-finish high deformation limit where the specimen is entirely in the M phase as shown in Fig. 1. By analogy, the following M+P full transformation on unloading should exhibit SMART phenomenology, if it is present in stress-induced transformations as well [11]:

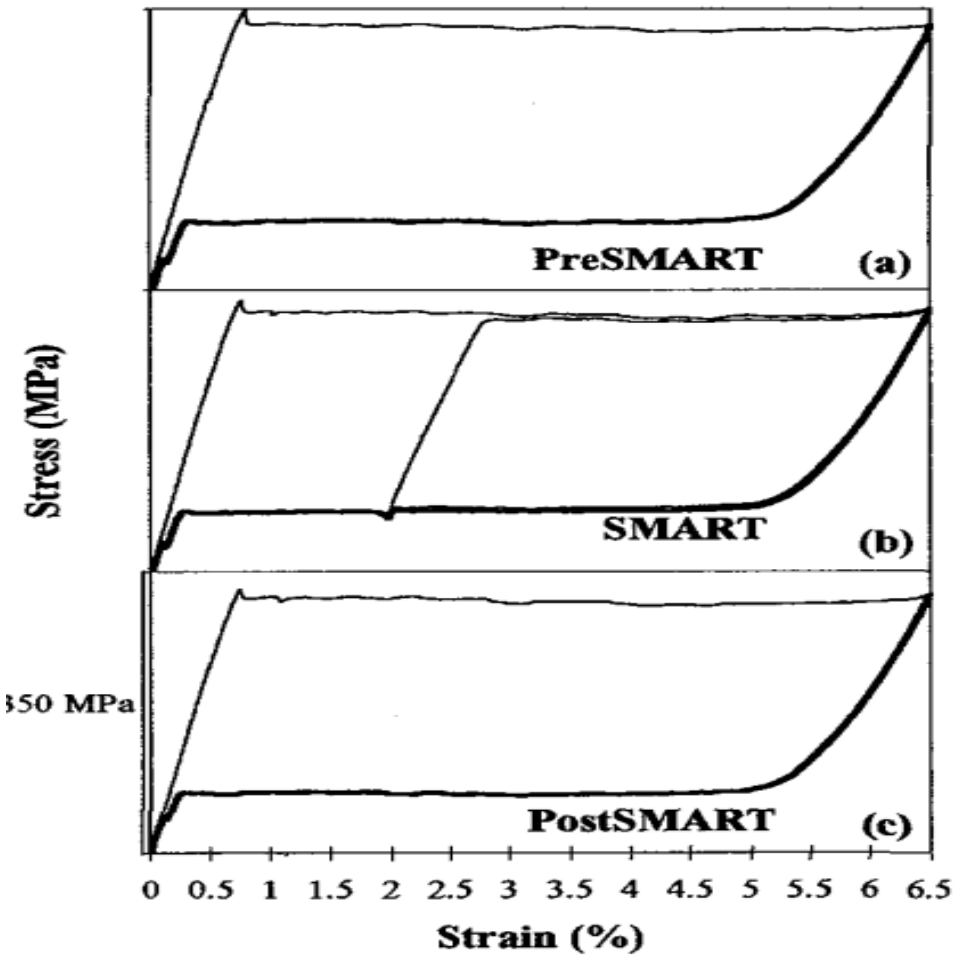

Figure 1: Stress Induced transformation Ib: (a) mechanical behavior before the procedure; (b) during SMART and (c) after SMART. In (b) the ICR cycle is also plotted [11].

The transition from Martensite (M) to Austenite (A) happens during heating, while the opposite transformation happens during cooling. The following basic equations represent such transformations as a function of temperature:

For heating:

$$\xi = \frac{\xi_m}{1+\exp\left[\frac{6.2}{Af-As}\left(T-\frac{As+Af}{2}\right)\right]} \quad \text{..... 1}$$

While for cooling:

$$\xi = \frac{1-\xi_A}{1+\exp\left[\frac{6.2}{Mf-Ms}\left(T-\frac{Ms+Mf}{2}\right)\right]} + \xi_A \quad \text{..... 2}$$

where ξ_m is the highest martensite fraction during cooling, ξ_A is the initial value of the martensite fraction during cooling, and As and Af are the initial and final temperatures of austenite transformation, respectively. M_s and M_f are the initial and final temperatures of martensite transformation, respectively. As = 68°C, A = 78°C, M = 52 °C, and M = 42°C are typical values. These values, however, could vary by up to ±15°C. To determine the accurate values for the wire used in the experimental actuator, an identification process will be utilized. Figs. 2, 3, 4 and 5 illustrate phase transition and make hysteresis clear. [12] [13]:

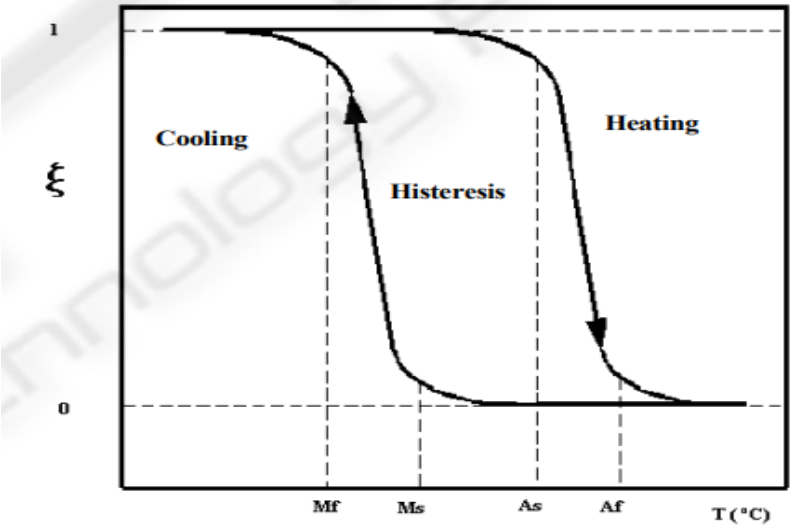

Figure 2: NiTi SMA phase transformation plot [12].

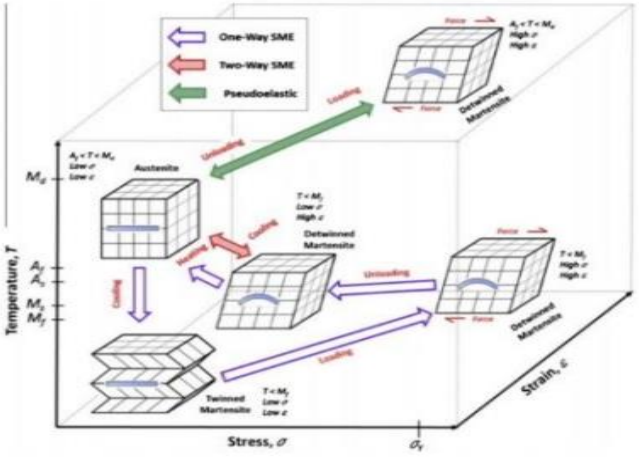

Figure 3: Crystal structures and Phases [14]

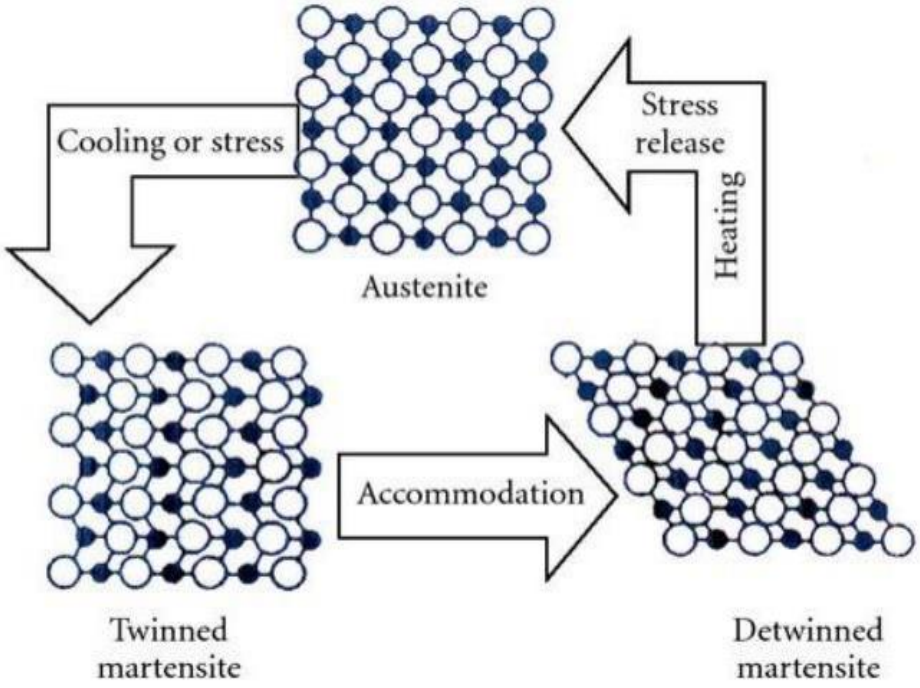

Figure 4: Phase transformation of SMA [14]

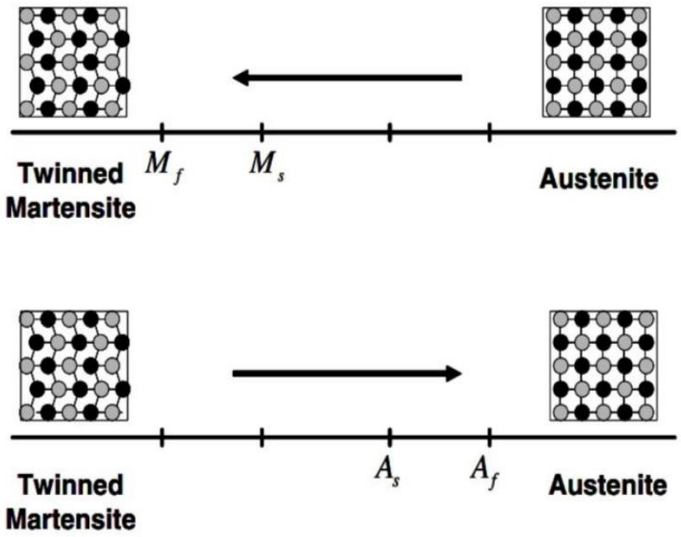

Figure 5: Structural change of SMA [14]

Nitinols Preparation Methods

Ni-Ti-SMA classified in the smart functional materials group. The significant characteristics of thermal shape memory effect exhibited by this group. After heating above a specific temperature (A_f the austenitic finish temperature) the alloy recovers its programmed shape and superelastic (rubber-like) behavior (the alloy recovers its original shape after deformation to tensile strain as high as 8%). Both of these characteristics' relay on thermoelastic and reversible martensitic transformations [15], [16]. Fig. 6 below illustrates nitinol production (preparation) methods.

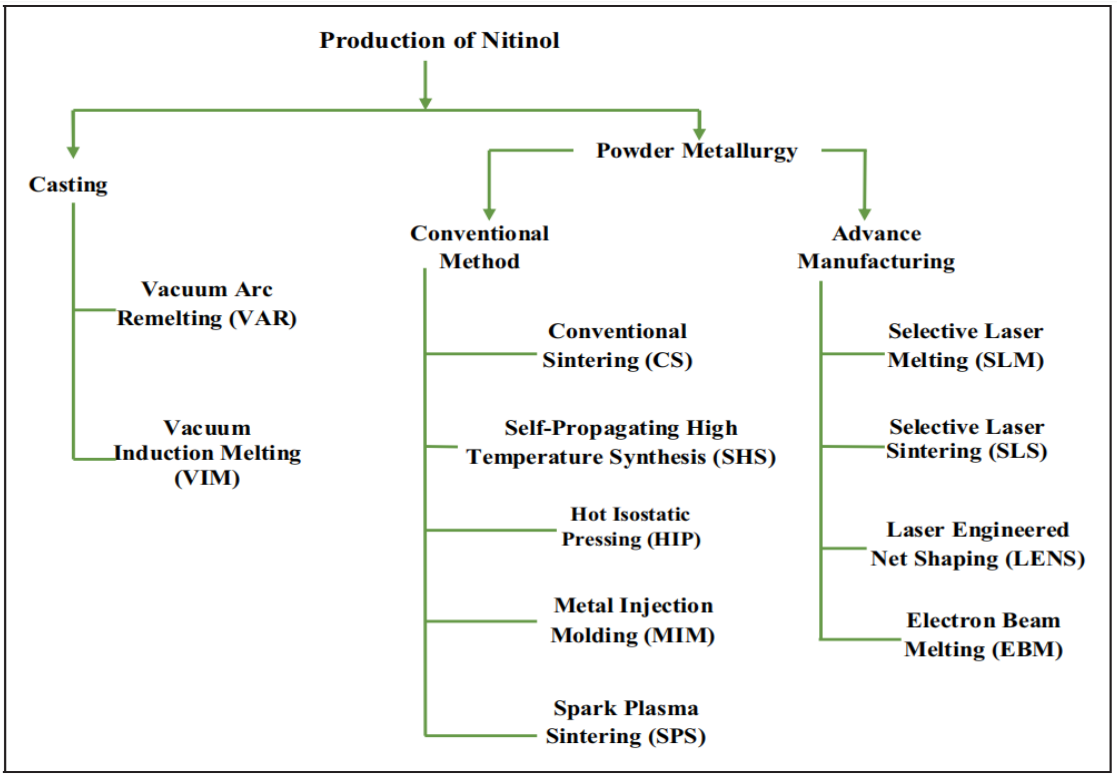

Figure 6: Nitinol Preparation Methods [17]

Pressure-assisted sintering, also known as hot pressing:

Master Samples NiTi (with or without additives such as Cu) prepared using powder mixture of Specific concentration (%) of Ni and Ti with or without additives by; mixing in a ball mill for two hours, then compacted at Specific pressure usually about 5 MPa, and then sintered at (950±50) °C for 9 hours under controlled atmosphere (argon) [15] [16] [18].

Conventional Sintering Method without pressure:
Master Samples NiTi (with or without additives such as Cu) prepared using powder mixture of Specific concentration (%) of Ni and Ti with or without additives by; mixing in a ball mill for two hours, and then sintered at (1250±50) °C for 9 hours under controlled atmosphere (argon) [15].

Selective Laser Melting (SLM) Technique:
The first step in the SLM process, sometimes called powder bed fusion, is to apply a thin layer of nitinol powder (thickness<100µm) on a substrate. The powder bed is then scanned by a high-power computer-controlled laser beam. By absorbing the laser beam's energy, the powder particles melt and solidify to create an input layer that is cross-sectional for a computer-aided design (CAD) model slice. With the aid of a spreader or recoater blade and an adjustable build platform, this process is repeated layer by layer until the entire item is constructed. [13].

Laser Engineered Net Shaping (LENS) Technique:
The building platform is bombed by a concentrated solid-state laser beam and used to melt the coaxially sprayed metal powder which solidifies in place [13].

Materials and Method
Experimental Procedure
Manufacturing Nitinol SMA alloy:
The nitinol shape memory alloy was manufactured locally in three different concentrations as follows:
1- 45% Ti + 55% Ni
2- 35% Ti + 45% Ni + 20% Al
3- 45% Ti + 35% Ni + 20% Cu

Raw Material Used in Manufacturing Nitinol SMA
For manufacturing the nitinol SMA, the required materials must be prepared as follows:
250 gm of Nickel (Ni) (70 micron).
1. 250 gm of Titanium (Ti) (44 micron).
2. 100 gm of fine powder Aluminum (Al) (about 60 micron).
3. 100 gm of fine powder Copper (Cu).

Melting Techniques:
In the precent experimental work two alloying techniques were used, they are:
1- Conventional sintering technique with argon for antioxidation.
2- Sintering technique which was include compacting the alloy at 5-ton pressure before melting.

Preparation principles:
The following criteria were used to calculate the melting point of each mixture after being compressed under five-ton pressure at a circular mold of 2mm thickness and 2cm diameter:
1. Nickel (Ni) melting point (M.P.) = 1455°C [19].
2. Titanium (Ti) M.P. = 1668°C [20][21].
3. Aluminum (Al) M.P. = 660°C [22]
4. Copper (Cu) M.P, = 1085°C [23]
5. Alloys of:

5.1 55% Ti + 45% Ni melting point (M.P.)
M.P.= (0.55×1668) + (0.45×1455) =1571.4°C
Sintering degree = 0.75 × M.P.= 0.75 × 1571.4°C = 1178.55°C, the sintering will be started at 1000°C and increased gradually according to need.

5.2 35% Ti + 45% Ni + 20% Al
M.P.= (0.35×1668) + (0.45×1455) + (0.2 × 660) =1370.55°C
Sintering degree = 0.75 × M.P.= 0.75 × 1370.55°C =1027.9°C, the sintering will be started at 900°C and increased gradually according to need.

5.3 45% Ti + 35% Ni + 20% Cu
M.P.= (0.45×1668) + (0.35×1455) + (0.2×1085) =1476.85°C
Sintering degree = 0.75 × M.P.= 0.75 × 1571.4°C = 1107°C, the sintering will be started at 950°C and increased gradually according to need.

Manufacturing procedure were done using the following equipments in the lab of college of material sciences in Al-Karkh university:
1- Materials weighing machine (four digits sensitive scale).
2- Magnetic steering.
3- Drying Alloy mixture using hot air oven.
4- Hydraulic Pressing the mixture, as in Fig. 10:

Figure 7: Hydraulic Presser

5- Graphite molds, Fig. 8 showing the graphite mold which contain three circular drilling designed by SolidWorks software and drilled using CNC machine of 2mm thickness and 2cm diameter to match samples dimensions. The mold contains three samples of nitinol compacted mixture, pure NiTi, NiTiCu, and NiTiAl.

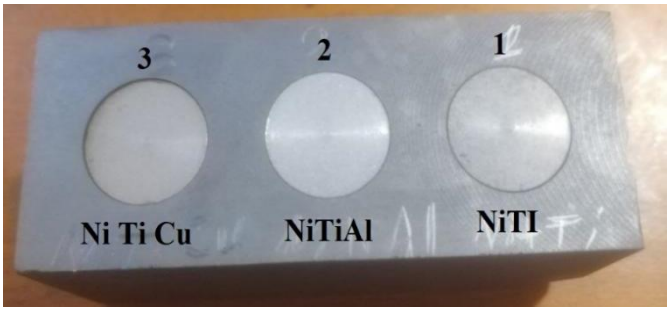

Figure 8: Samples in graphite mold before casting

6- Each sample were casted separately for 5 hours using the proper temperature estimated from the calculations explains previously, i.e., NiTi alloy melted at 1200°C, NiTiCu melted at 900°C, and NiTiAl alloy melted at 700°C. The casting procedure was done by using Argon gas as antioxidation agent.

Functional and structural laboratories tests:

Samples were tested for its structure identity by X-Ray diffraction analysis (XRD) test which is XRD is a valuable technique expose the crystallin structure and lattice parameters of material, energy dispersive spectroscopy (EDS) an analytical method that makes it possible to analyze a material's elements and chemical composition, scanning electron microscope (SEM) was used to investigate the microstructures of the samples conducted by means of SEM device with vacuum atmosphere field-emission scanning electron microscopy (FESEM); and for its function by differential scanning calorimetry (DSC) test. Testing equipment shown in Fig. 9, Fig. 10, and Fig. 11.

Figure 9: Shows XRD machine from Malvern Panalytical, model AERIS research edition

Figure 10: Shows EDS mapping machine from Thermoscientific company, model Axia ChemiSEM

Figure 11: Shows FESEM from FEI company, model Inspect™ F50

Results

Prepare and Fabricate (45% Ti + 55% Ni) Alloy

NiTi alloy prepared by sintering the raw material under five ton of pressure for five minutes and then melting the mixture in 1250°C for five hours with the help of argon gas to prevent oxidation. The resulted alloy acts as SMA.

A. Structural tests

Identifying the resulted alloy structural composition was identified using XRD test, EDS test, and SEM test which exposed the results as shown in Tables 2 and 3, Fig. 12, Fig. 13, and Fig. 14.

Name and formula for XRD test was:

1- Reference code: 96-152-2996.
2- Compound name: (Ni0.906 Ti0.094).
3- Common name: (Ni0.906 Ti0.094)
4- Chemical formula: Ni3.64Ti0.36

Crystallographic parameters show that:

1- Crystal system: Cubic
a- (Å): 3.5560
b- (Å): 3.5560
c- (Å): 3.5560
2- Calculated density (g/cm^3): 8.53
3- Volume of cell (106 pm^3): 44.97

The X-ray inspection findings of a pure nickel titanium alloy are displayed in Table 2. The values of the inter-angle distance (d) and the coefficients (h, k, and l) related to the diffraction angle demonstrate that when

2θ→ (h, k, l)1,1,1→ d=2.035Å
2θ→ (h, k, l) 0,2,0→ d=1.778 Å
2θ→ (h, k, l)0,2,2→ d=1.257Å

The X-ray image of the pure nickel titanium alloy is shown in Fig.12, where regular crystallization is observed as the sintering temperature increases. The alloy's volume of the crystal cell is 44.96 pm^3 cubed, indicating that it is in the cubic crystal structure with a density of 8.53 gm/cm^3 centimeter. These results including high density due to compact the powder mixture under high pressure (5 ton) and sintering under high temperature (1250°C) for long period (5 hours) which increase the density and decrease the porosity of the alloy comparing to Tianhu Miao, Sha Zhan, Xiaojuan Chen et al. at 2024 in their article (Effect of Sintering Temperature on microstructure Characteristics of Porous NiTi Alloy Fabricated via Elemental Powder Sintering) whom get a density of 2.556 g/cm^3 to 3.030 g/cm^3 after sintering in 950°C and 1000°C respectively for four hours without compact the mixture while matching in our and their study in getting three diffraction peaks at 2 θ angles of about 44.49°, 51.84° and 76.37° with a face-centered cubic crystal structure which is similar to this study results [24].

Table 2: Peak, angle, and spacing values for NiTi alloy

No.	H	K	l	Height [cts]	Pos. [°2θ]	d-spacing [Å]
1.	1	1	1	9905.18	44.073	2.05306
2.	0	2	0	839.86	51.347	1.77800
3.	0	2	2	2841.28	75.569	1.25724

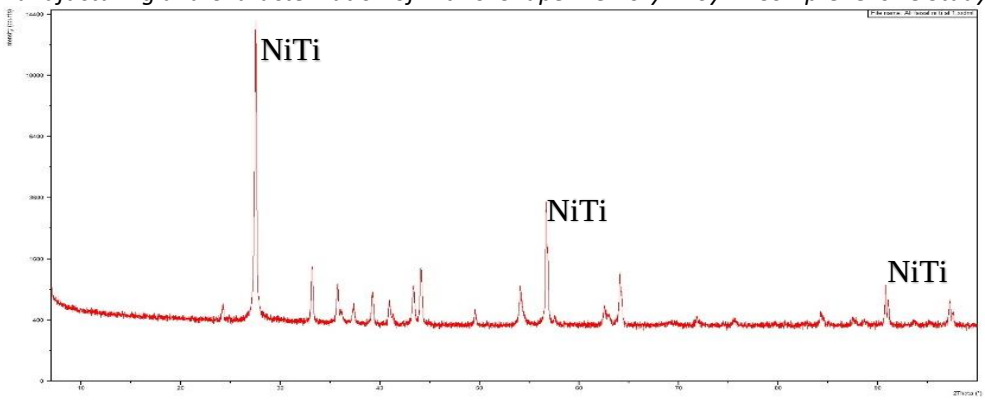

Figure 12: Shows X-ray diffraction pattern for resulted NiTi alloy

Table 3 below presents the EDS values obtained from the SEM test of the pure NiTi alloy. The percentages of nickel (54.4%) and titanium (44.6%) in the alloy clearly indicate its purity, indicating that the concentrations utilized in the alloy's practical production are in line with the test findings.

Table 3: Percentage of atomic concentration and weight of NiTi alloy

Element	Atomic %	Atomic % Error	Weight %	Weight % Error
Ti	37.3	0.2	54.4	0.3
Ni	0.4	0.0	44.6	0.1

The pure NiTi alloy's EDX energy spectroscopic pattern is displayed in Fig. 13 (a) and (b). The titanium intensity values in this pattern are higher than those of the nickel material, showing that the alloy's preparation technique is consistent with the test results. Furthermore, the development of NiTi alloy clusters is depicted in the SEM image shown in Figure 14.

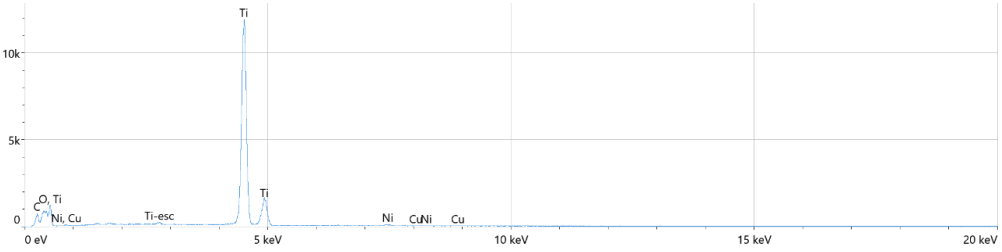

(a)

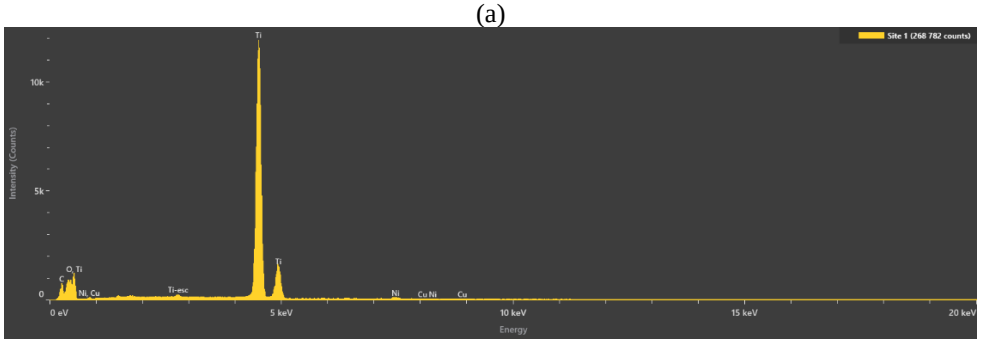

(b)

Figure 13: EDS image of NiTi alloy

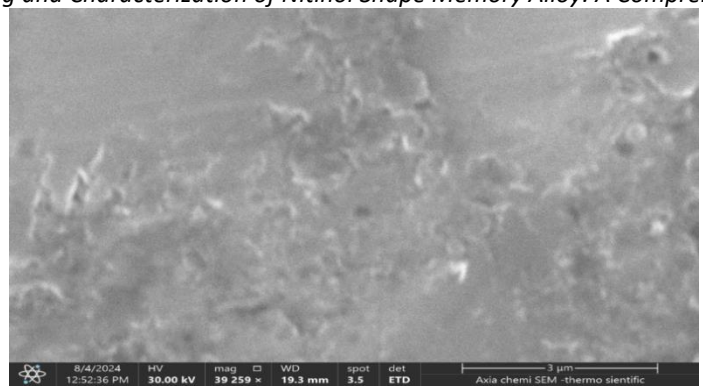

Figure 14: High magnification FESEM images showing variations in surface asperities formed on NiTi alloy

B. Differential (functional) test (DSC):

The resulted alloy acts as SMA. Differential scanning calorimetry (DSC) test explain the properties of this alloy as shown in Fig. 15. The curve for each data set indicates an endothermic transformation event, signifying a transition to a martensitic and an austenitic microstructure. Two phase of heating transformation temperature were shown: A_s at 60.87 °C and A_f at 75.40 °C, and A_s at 292.87°C and A_f at 358.19°C which is 10°C higher than Rodolfo da Silva Teixeira, Rebeca Vieira de Oliveira, Patrícia Freitas Rodrigues et al. at 2022 in their article (Microwave versus Conventional Sintering of NiTi Alloys Processed by Mechanical Alloying) whom sintering their samples at 850 ◦C for 120 min, and the resulted alloy had A_f of 58.3°C [25].

Where A_s: Austenitic starting temperature, A_f: Austenitic finishing temperature.

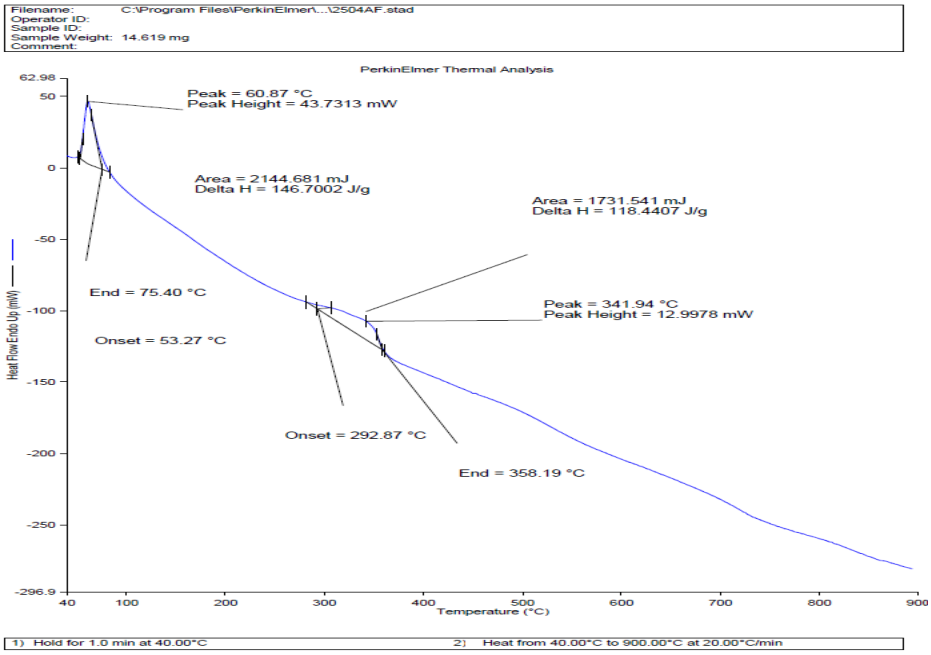

Figure 15: Calorimetry (DSC test) curves obtained upon heating samples cut from various location of the NiTi alloy.

Prepare and Fabricate (45% Ti + 35% Ni + 20% Cu):

NiTiCu alloy prepared by sintering the alloy under five ton of pressure for five minutes and then melting the mixture in 950°C for five hours with the help of argon gas to prevent oxidation.

A. Structural tests

Identifying the resulted alloy structural composition was identified using XRD test, EDS test, and SEM test which exposed the results as shown in Tables 4, 5, and Fig. 16 to Fig. 21.

Name and formula for XRD test was:

Reference code for XRD: 96-152-5298.

1- Compound name: (Cu0.03 Ni0.97)3 Ti
2- Common name: (Cu0.03 Ni0.97)3 Ti
3- Chemical formula was: Cu0.90Ti10.00Ni29.10

While Crystallographic parameters show that:

1- Crystal system: Hexagonal
a- (Å): 5.1160
b- (Å): 5.1160
c- (Å): 20.9000
2- Calculated density (g/cm3): 7.87
3- Volume of cell (106 pm3): 473.74

The copper-doped nickel-titanium alloy's X-ray analysis findings are displayed above shows that the density of the

NiTiCu alloy is 7.87 g/cm^3, which is smaller than the 8.789 g/cm^3 of the pure nickel-titanium alloy that was previously displayed. This is a result of the copper atom being present in this alloy's crystal structure.

The X-ray inspection findings of the NiTiCu alloy are displayed in Table 4. The values of the inter-angle distance (d) and the coefficients (h, k, and l) related to the diffraction angle demonstrate that when

2θ→ (h, k, l) 1,0,4→ d=3.28120Å
2θ→ (h, k, l) 1,0,9→ d=2.05852 Å
2θ→ (h, k, l) 2,0,7→ d=1.78121Å

Table 4: Peak, angle, and spacing values for NiTiCu alloy

No.	h	k	l	Height [cts]	Pos. [°2θ]	d-spacing [Å]
1.	1	0	4	872.14	27.1551	3.28120
2.	1	0	9	1881.47	43.9497	2.05852
3.	2	0	7	756.75	51.2474	1.78121

Table 5 presents the EDS values obtained from the SEM test of the NiTiCu alloy. The percentages weight of nickel (32.0%), titanium (50.1%), and the cupper (17.9%) in the NiTiCu alloy, indicating that the concentrations utilized in the alloy's practical production are in line with the test findings. The Table also indicate an error percentage resulted from testing techniques.

Table 5: Percentage of atomic concentration and weight of NiTi alloy

Element	Atomic %	Atomic % Error	Weight %	Weight % Error
Ti	47.3	0.3	50.1	0.3
Ni	37.1	0.2	32.0	0.2
Cu	15.6	0.3	17.9	0.3

Fig. 16 shows the standard X-ray diffraction pattern of the nickel-titanium-copper alloy, which is consistent with the X-ray diffraction pattern of the nickel-titanium-copper alloy prepared in this study, as shown in Figure 17.

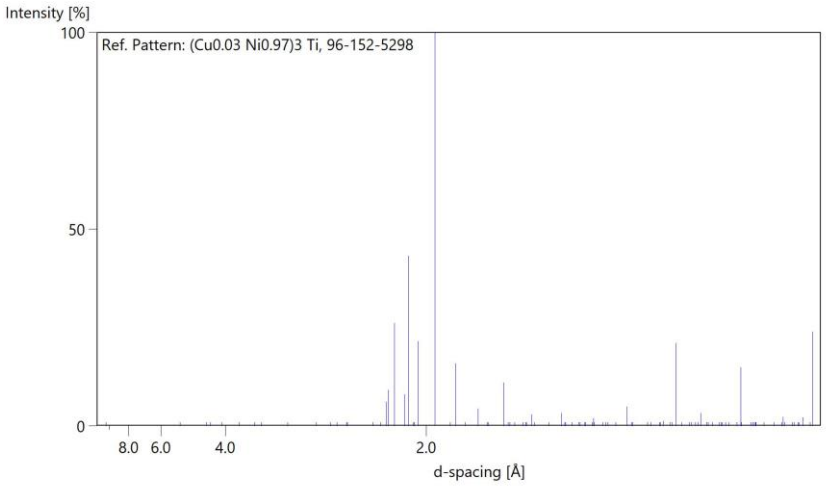

Figure 16: Standard diffraction for NiTiCu alloy.

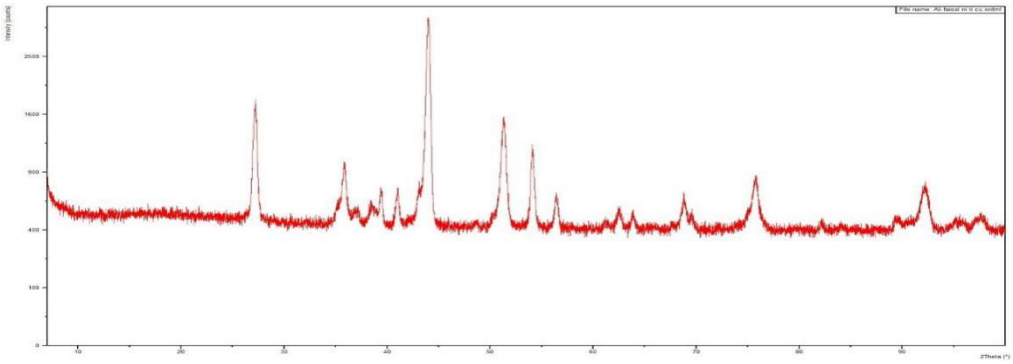

Figure 17: Shows X-ray diffraction pattern for resulted NiTiCu alloy

The NiTiCu alloy's EDX energy spectroscopic pattern is displayed in Fig. 18 (a) and (b). The titanium intensity values in this pattern are higher than those of the nickel material, showing that the alloy's preparation technique is consistent with the test

results. Furthermore, the development of NiTi alloy clusters is depicted in the SEM image shown in Fig. 19, Fig. 20-a, b, c) and Fig. 21-a, b).

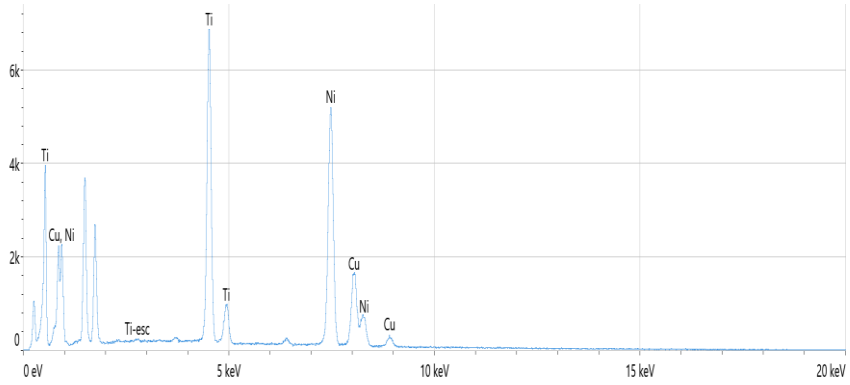

(a)

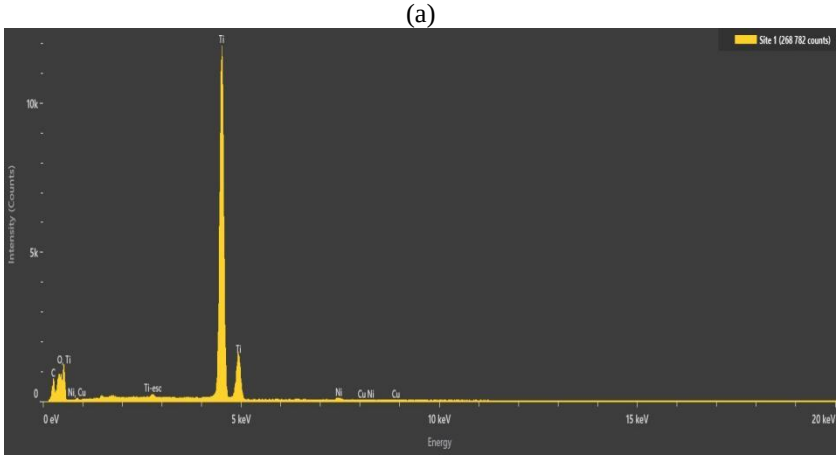

(b)

Figure 18: EDS image of NiTi alloy

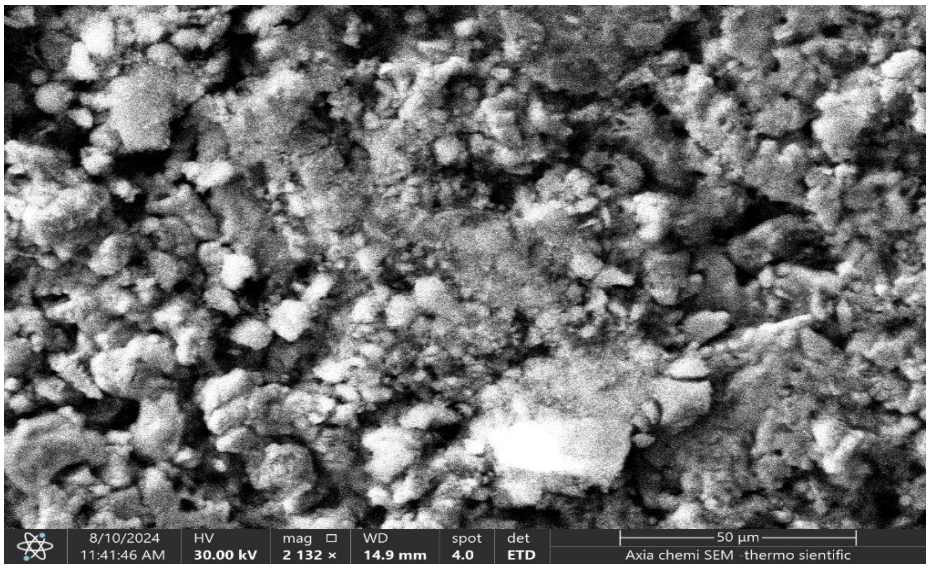

Figure 19: SEM scanning image for NiTiCu Alloy shows the alloy composition

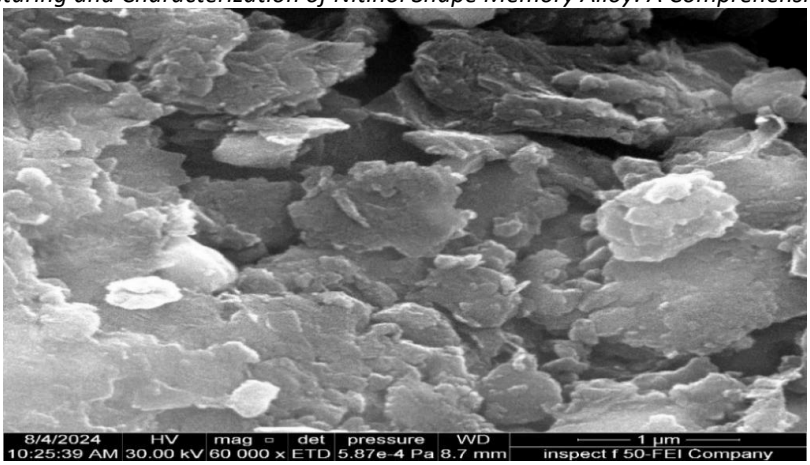

(a)

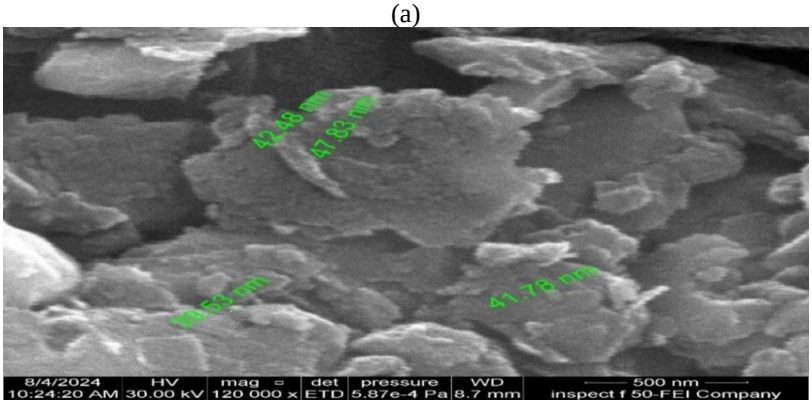

(b)

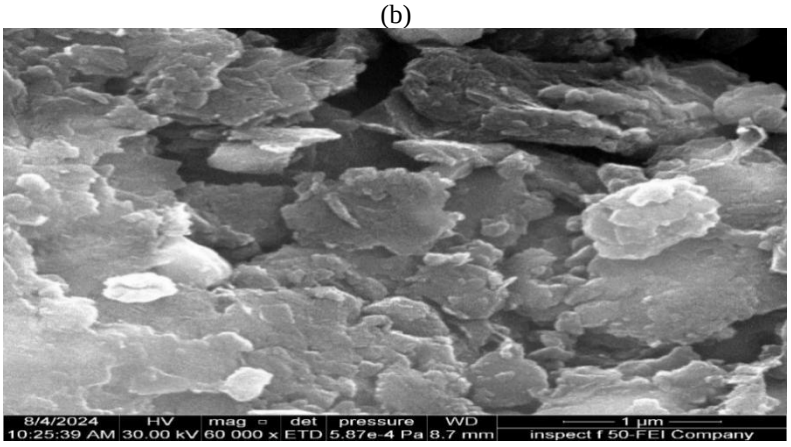

(c)

Figure 20: Different FESEM micrographs illustration of NiTiCu alloy

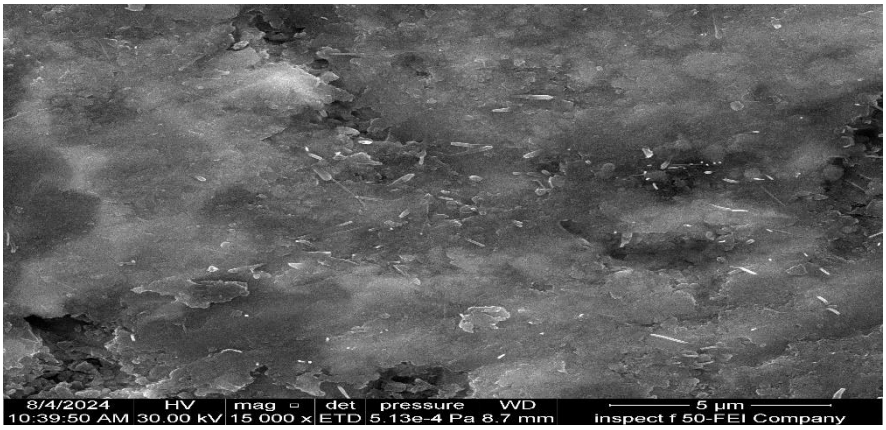

(a)

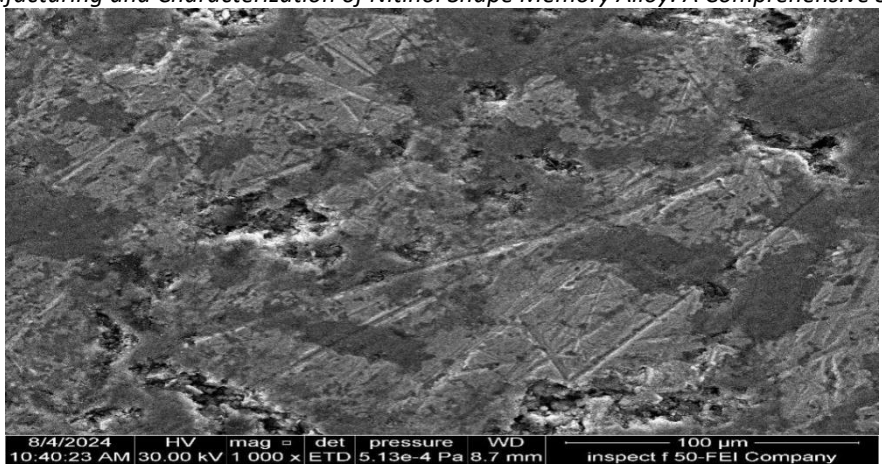

(b)

Figure 21: Different high magnification FESEM images showing variations in surface asperities formed on NiTiCu alloy in different microstructural sizes

B. Differential (functional) test (DSC):

Differential scanning calorimetry (DSC) test explain the properties of this alloy as shown in Fig. 22. The curve for each data set indicates an endothermic transformation event, signifying a transition to an austenitic microstructure. Two phase of heating transformation temperature were shown: As at 60.57 °C and A_f at 69.69 °C, and As at 115.03°C and A_f at 135.8°C.

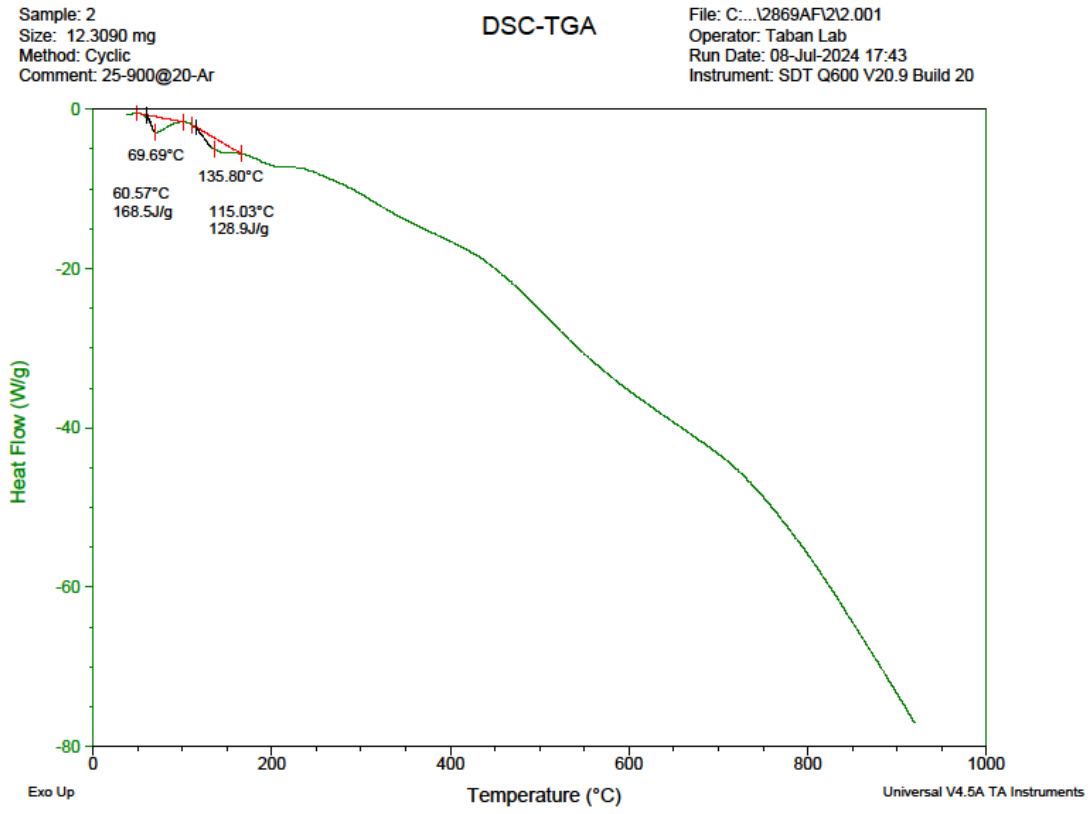

Figure 22: Calorimetry (DSC test) curves obtained upon heating samples cut from various location of the NiTiCu alloy.

Prepare and Fabricate (35% Ti + 45% Ni + 20% Al) Alloy

NiTiAl alloy prepared by sintering the raw material under five ton of pressure for five minutes and then melting the mixture in 750°C for five hours with the help of argon gas to prevent oxidation. The resulted alloy acts as SMA.

A. Structural tests

Identifying the resulted alloy structural composition was identified using XRD test, EDS test, and SEM test which exposed the results as shown in Tables 6 and 7, Fig. 23 to Fig. 26.

Name and formula for XRD test was:

1- Reference code: 96-153-3506

2- Compound name: Ti27.55 Ni28 Al63.73
3- Common name: Ti27.55 Ni28 Al63.73
4- Chemical formula: Al63.73Ti27.55Ni28.00

While the crystallographic parameters are:
1- Crystal system: Cubic
a- (Å): 11.8930
b- (Å): 11.8930
c- (Å): 11.8930
2- Calculated density (g/cm3): 4.62
3- Volume of cell (106 pm3): 1682.19

The aluminum-doped nickel-titanium alloy's X-ray analysis findings are displayed above shows that the density of the NiTiAl alloy is 4.62 g/cm^3, which is smaller than the 8.789 g/cm^3 of the pure NiTi and smaller than 7.87g/cm^3 of the NiTiCu alloy that was previously displayed. There is a change in the crystallin structure of the alloy as a result of the low density of the added aluminum element and the difference in the (d) values from the other two alloys

The X-ray inspection findings of the NiTiCu alloy are displayed in Table 6. The values of the inter-angle distance (d) and the coefficients (h, k, and l) related to the diffraction angle demonstrate that when

2θ→ (h, k, l) 2,4,2→ d=2.39773Å
2θ→ (h, k, l) 0,4,4→ d=2.08169Å
2θ→ (h, k, l) 1,5,3→ d=1.99945Å

Table 6: Peak, angle, and spacing values for NiTiAl alloy

No.	h	k	l	Height [cts]	Pos. [°2θ]	d-spacing [Å]
1.	2	4	2	696.12	37.4784	2.39773
2.	0	4	4	753.99	43.4355	2.08169
3.	1	5	3	677.15	45.3192	1.99945

Table 7 below presents the EDS values obtained from the SEM test of the NiTiCu alloy. The percentages weight of nickel (30.4%), titanium (41.5%), and the aluminum (12.6%) in the NiTiCu alloy, indicating that the concentrations utilized in the alloy's practical production are in line with the test findings. The Table also indicate a small error percentage resulted from testing techniques.

Table 7: Percentage of atomic concentration and weight of NiTiAl alloy

Element	Atomic %	Atomic % Error	Weight %	Weight % Error
Al	8.1	0.1	12.6	0.1
Ti	8.2	0.0	41.5	0.1
Ni	10.2	0.0	30.4	0.1
O	0.2	0.0	8.5	
CU	0.5	0.0	3.0	

Fig. 23 shows the standard X-ray diffraction pattern of the NiTiAl alloy, which is consistent with the X-ray diffraction pattern of the NiTiAl alloy prepared in this study, as shown in Fig. 24.

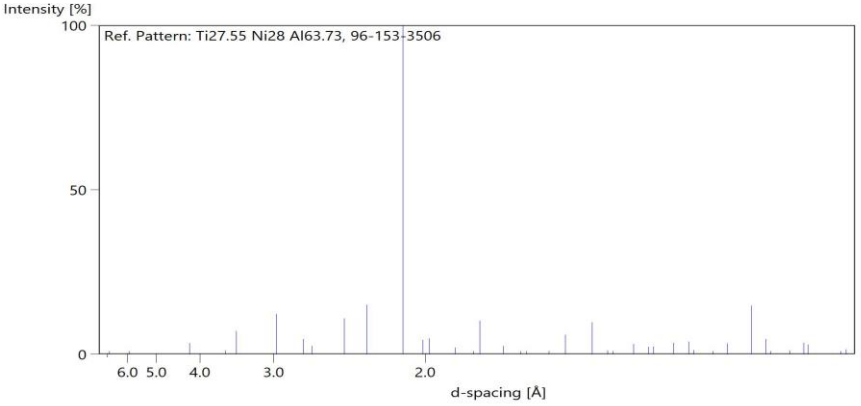

Figure 23: Standard XRD diffraction for NiTiAl alloy

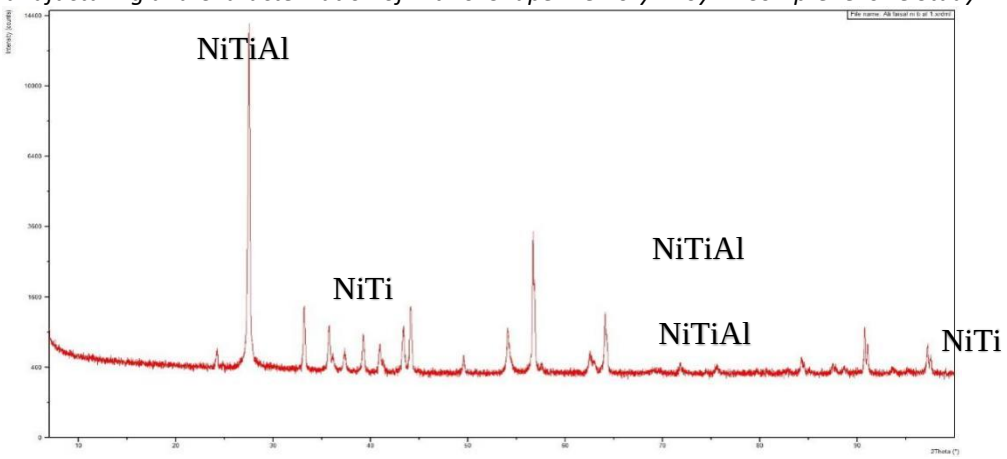

Figure 24: Shows XRD diffraction pattern for manufactured NiTiAl alloy

The NiTiAl alloy's EDX energy spectroscopic pattern is displayed in Fig. 25 (a) and (b). The titanium intensity values in this pattern are higher than those of the nickel material, showing that the alloy's preparation technique is consistent with the test results. Furthermore, the development of NiTi alloy clusters is depicted in the SEM image shown in Fig. 26.

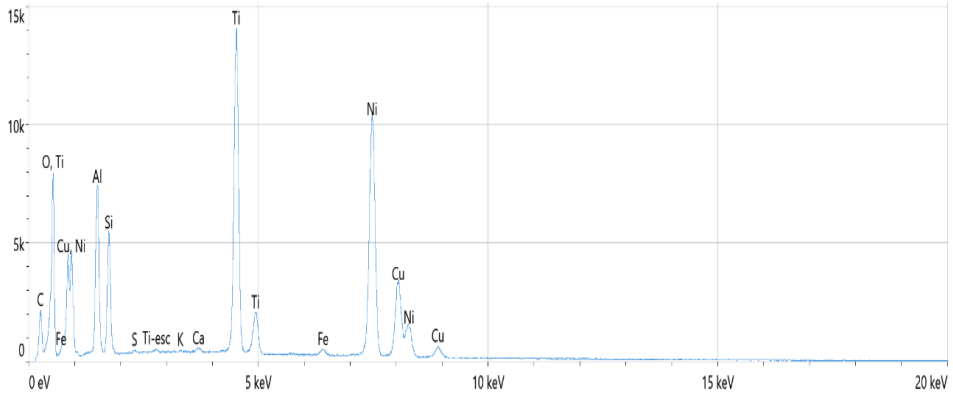

(a)

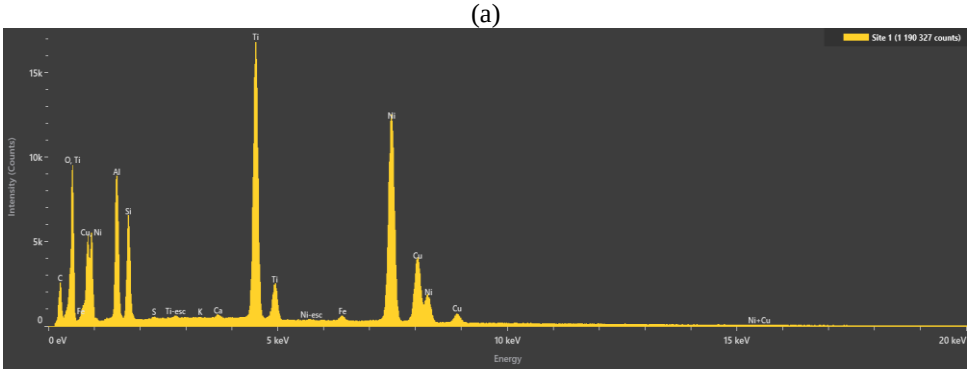

(b)

Figure 25: EDS image of NiTiAl alloy

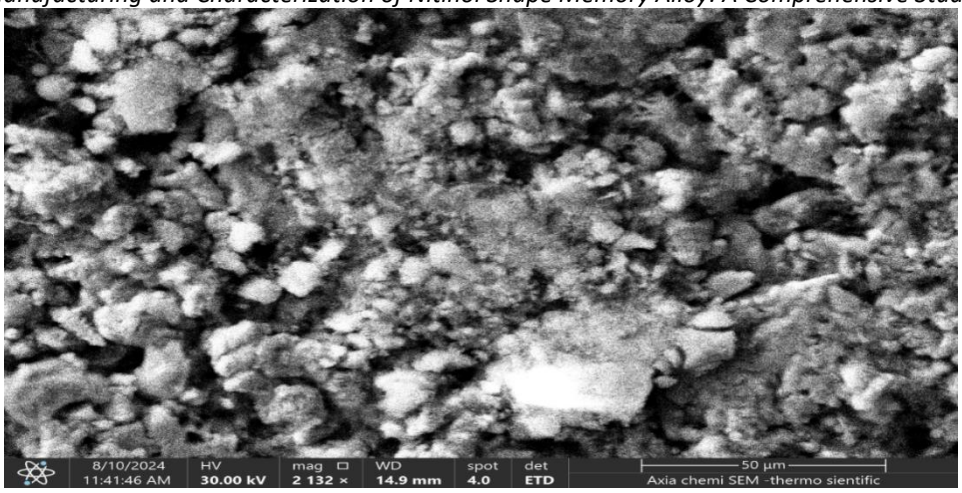

Figure 26: High magnification FESEM images showing variations in surface asperities formed on NiTiAl alloy

B. Differential (functional) test (DSC):

Differential scanning calorimetry (DSC) test explain the properties of this alloy as shown in Fig. 27. The curve for each data set indicates an endothermic transformation event, signifying a transition to an austenitic microstructure. Two phase of heating transformation temperature were shown: As at 64.10 °C and Af at 75.03 °C, and As at 122.97°C and Af at 142.96°C.

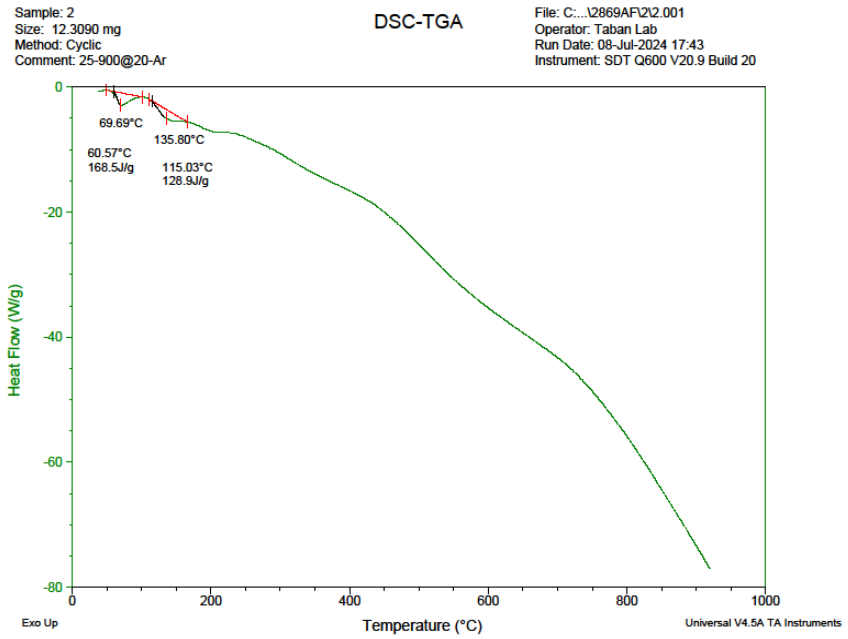

Figure 27: Calorimetry (DSC test) curves obtained upon heating samples cut from various location of the NiTiAl alloy.

Preparing SMA Use Conventional Melting Technique:

All the alloy mixture prepared using this technique (i.e., NiTi, NiTiAl, NiTiCu) did not succeed. Several trails used for each mixture and the sample either burned or failed to melt.

Discussion

NiTi Alloy

This alloy has moderate transformation temperature (Transformation temperature Ms at 60.87 °C and Mf at 292.87 °C, and As at 292.87°C and Af at 358.19°C.) compared to the NiTiCu SMA alloy and NiTiAl alloy because of low molecular weight additives in the last two alloys results in smaller transformation temperatures.

NiTiCu Alloy

This alloy has the highest transformation temperature (Transformation temperature As at 60.57 °C and Af at 69.69 °C, and As at 115.03°C and Af at 135.8°C.). This alloy was the most important for this study because this study aims to prepare NiTiCu alloy from the same composition used in the NiTiCu SMA wires utilized in the insole fabricated in this study. The goal is to prepare a suitable transformation temperature more than 30°C to mimic expected foot temperature while walking in high temperature atmospheric weather and high activity of children. This alloy achieves the requirement with transformation temperature more than required because of that NiTiCu 2mm thickness plate alloy have heat capacity more than 0.5mm diameter NiTiCu SMA wire. To reduce transformation

temperature and keep high reshaping SMA force effect it is needed to reduce thickness and increase Cu impurities of the alloy to the right balance.

NiTiAl Alloy

This alloy has the lower transformation temperature (As at 64.10 °C and Af at 75.03 °C, and As at 122.97°C and Af at 142.96°C) compared to the previous fabricated alloys because of aluminum additives results in reducing transformation temperature of the nitinol mixture.

Although the structurally and functionally tested part indicates the success of the alloy, practically most of the samples was either burned or not melted. This is due to the fact that aluminum has a low melting point compared to nickel and titanium, which requires reducing its proportion to avoid burning.

While this study alloy use sintering and melting for five hours, other studies use other technique that needs more advance technology such as additive material manufacturing technique[26] [27], thermal explosion mode of self-propagating high-temperature synthesis (TE-SHS) technique [28], powder metallurgy techniques [29], or selective laser melting technique [30][17]. It must be mentioned that (DSC) test start at 40°C which did not give a clear view about tis alloy action at smaller temperature. Unfortunately, DSC test was not available for metal samples in other conditions neither locally in Iraq nor in the surrounding countries.

Fabricating Nitinol SMA Using Conventional Melting Technique

This Technique failed in this study for all type of nitinol concertation. The reason of that may be because of limited available melting time. Most study mention eight hours of melting time which couldn't be achieved in this study.

Conclusion:

This study concludes that manufacturing nitinol alloy by sintering method after compressing the raw material mixture can be a proper technique and changing the concentration of mixture raw material can affect the shape memory alloy transformation temperatures including austenitic transformation phase and martensitic transformation phase.

References

Bouaissi, A.; Radhi, N.S.; Morad, K.F.; Hafiz, M.H.; Atiyah, A.A. OPTIMIZATION OF NICKEL CONTENT ON SOME PROPERTIES OF (NITI) SHAPE MEMORY ALLOY. *Knowledge-Based Engineering and Sciences* 2020, *1*, 40–47, doi:10.51526/kbes.2020.1.01.40-47.

Behera, A. Smart Applications of NiTi Shape Memory Alloy in Biomedical Industries. In *Nickel-Titanium Smart Hybrid Materials: From Micro- to Nano-structured Alloys for Emerging Applications*; Elsevier, 2022; pp. 327–354 ISBN 9780323911733.

Otsuka, K.; Ren, X. Physical Metallurgy of Ti-Ni-Based Shape Memory Alloys. *Prog Mater Sci* 2005, *50*.

Huibin, X.U. Temperature Hysteresis in Shape Memory Alloys. *Chinese Physics Letters* 1991, *8*, 251–254, doi:10.1088/0256-307X/8/5/010.

Duerig, T.; Pelton, A.; Stöckel, D. An Overview of Nitinol Medical Applications. *Materials Science and Engineering: A* 1999, *273–275*, 149–160, doi:10.1016/s0921-5093(99)00294-4.

Pelton, A.R.; Stöckel, D.; Duerig, T.W. Medical Uses of Nitinol. *Materials Science Forum* 2000, *327*, 63–70, doi:10.4028/www.scientific.net/msf.327-328.63.

Kapoor, D. Nitinol for Medical Applications: A Brief Introduction to the Properties and Processing of Nickel Titanium Shape Memory Alloys and Their Use in Stents. *Johnson Matthey Technology Review* 2017, *61*, 66–76.

Safranski, D.; Dupont, K.; Gall, K. Pseudoelastic NiTiNOL in Orthopaedic Applications. *Shape Memory and Superelasticity* 2020, *6*, 332–341, doi:10.1007/s40830-020-00294-y.

Schipper, O.N.; Ellington, J.K. Nitinol Compression Staples in Foot and Ankle Surgery. *Orthopedic Clinics of North America* 2019, *50*, 391–399.

JORDAN, L.; GOUBAA, K.; MASSE, M.; BOUQUET, G. COMPARATIVE STUDY OF MECHANICAL PROPERTIES OF VARIOUS Ni-Ti BASED SHAPE MEMORY ALLOYS IN VIEW OF DENTAL AND MEDICAL APPLICATIONS. *Le Journal de Physique IV* 1991, *01*, C4-139-C4-144, doi:10.1051/jp4:1991421.

Airoldi, G.; Corsi, A.; Riva, G. The Step-Wise Martensite to Austenite Reversible Transformation Stimulated by a Stress State. *Journal De Physique. IV : JP* 1997, *7*, doi:10.1051/jp4:1997581.

Romano, R.; Tannuri, E.A. New Development on Shape Memory Alloys Actuators. In Proceedings of the BIODEVICES 2008 - Proceedings of the 1st International Conference on Biomedical Electronics and Devices; 2008; Vol. 2, pp. 55–61.

Chekotu, J.C.; Groarke, R.; O'Toole, K.; Brabazon, D. Advances in Selective Laser Melting of Nitinol Shape Memory Alloy Part Production. *Materials* 2019, *12*.

Balasubramanian, M.; Srimath, R.; Vignesh, L.; Rajesh, S. Application of Shape Memory Alloys in Engineering - A Review. In Proceedings of the Journal of Physics: Conference Series; IOP Publishing Ltd, October 25 2021; Vol. 2054.

Drossou-Agakidou, V.; Kanakoudi-Tsakalidou, F.; Sarafidis, K.; Taparkou, A.; Tzimouli, V.; Tsandali, H.; Kremenopoulos, G. ASM Handbook Volume 2: Properties and Selection: Nonferrous Alloys and Special-Purpose Materials. ASM International Handbook Committee. *Eur J Pediatr* 1990, *157*.

R. Areef, S. Characterization of Ni-Ti Shape Memory Alloys. *Engineering and Technology Journal* 2010, *28*, 992–1000, doi:10.30684/etj.28.5.11.

Sharma, N.; Jangra, K.K.; Raj, T. Fabrication of NiTi Alloy: A Review. *Proceedings of the Institution of Mechanical Engineers, Part L: Journal of Materials: Design and Applications* 2018, *232*, 250–269.

Novák, P.; Moravec, H.; Salvetr, P.; Průša, F.; Drahokoupil, J.; Kopeček, J.; Karlík, M.; Kubatík, T.F. Preparation of Nitinol by Non-Conventional Powder Metallurgy Techniques. *Materials Science and Technology (United Kingdom)* 2015, *31*, doi:10.1179/1743284715Y.0000000041.

Jordan, L.; Swanger, W.H. The Properties of Pure Nickel. *Bureau of Standards Journal of Research* 1930, *5*, 1291, doi:10.6028/jres.005.075.

PIERRE, P.D.S.S. A Note on the Melting Point of Titanium Dioxide. *Journal of the American Ceramic Society* 1952, *35*, 188–188, doi:10.1111/j.1151-2916.1952.tb13097.x.

Niinomi, M. Recent Research and Development in Titanium Alloys for Biomedical Applications and Healthcare Goods. *Sci Technol Adv Mater* 2003, *4*, 445–454.

Cobden, R.; Banbury, A. Aluminium: Physical Properties, Characteristics and Alloys. *Talal* 1994, 60, doi:1994.
Li, M.; Zinkle, S.J. 4.20 - Physical and Mechanical Properties of Copper and Copper Alloys. In *Comprehensive Nuclear Materials: Volume 1-5*; Elsevier, 2012; Vol. 1–5, pp. 667–690 ISBN 9780080560335.
Miao, T.; Zhan, S.; Chen, X.; Hu, L. Effect of Sintering Temperature on Microstructure Characteristics of Porous NiTi Alloy Fabricated via Elemental Powder Sintering. *Materials* 2024, *17*, doi:10.3390/ma17030743.
Teixeira, R. da S.; Oliveira, R.V. de; Rodrigues, P.F.; Mascarenhas, J.; Neves, F.C.F.P.; Paula, A. dos S. Microwave versus Conventional Sintering of NiTi Alloys Processed by Mechanical Alloying. *Materials* 2022, *15*, doi:10.3390/ma15165506.
Walker, J.M. Additive Manufacturing towards the Realization of Porous and Stiffness-Tailored NiTi Implants. *PhD Dissertation: The University of Toledo* 2014, 180.
Sathishkumar, M.; Kumar, C.P.; Ganesh, S.S.S.; Venkatesh, M.; Radhika, N.; Vignesh, M.; Pazhani, A. Possibilities, Performance and Challenges of Nitinol Alloy Fabricated by Directed Energy Deposition and Powder Bed Fusion for Biomedical Implants. *J Manuf Process* 2023, *102*, 885–909.
Čapek, J.; Kučera, V.; Fousová, M.; Vojtech, D. Preparation of the NiTi Shape Memory Alloy by the TE-SHS Method - Influence of the Sintering Time. In Proceedings of the METAL 2013 - 22nd International Conference on Metallurgy and Materials, Conference Proceedings; TANGER Ltd., 2013; pp. 1323–1327.
Novák, P.; Moravec, H.; Salvetr, P.; Průša, F.; Drahokoupil, J.; Kopeček, J.; Karlík, M.; Kubatík, T.F. Preparation of Nitinol by Non-Conventional Powder Metallurgy Techniques. *Materials Science and Technology (United Kingdom)* 2015, *31*, 1886–1893, doi:10.1179/1743284715Y.0000000041.
Walker, J.; Elahinia, M.; Haberland, C. An Investigation of Process Parameters on Selective Laser Melting of Nitinol. In Proceedings of the ASME 2013 Conference on Smart Materials, Adaptive Structures and Intelligent Systems, SMASIS 2013; American Society of Mechanical Engineers, 2013; Vol. 1.